RESEARCH ARTICLE | JANUARY 19 2024

Synthesis and characterisation of hydroxyapatite from *Fringescale sardinella* for biomedical applications

Mohamed Saiful Firdaus Hussin; Maizlinda Izwana Idris ✉; Hasan Zuhudi Abdullah; Al Amin Mohamed Sultan

AIP Conf. Proc. 2925, 020045 (2024)
https://doi.org/10.1063/5.0183935

Synthesis and Characterisation of Hydroxyapatite from *Fringescale Sardinella* for Biomedical Applications

Mohamed Saiful Firdaus Hussin[1, 2, b)], Maizlinda Izwana Idris[1, a)], Hasan Zuhudi Abdullah[1, c)] and Al Amin Mohamed Sultan[3, d)]

[1]*Faculty of Mechanical and Manufacturing Engineering, Universiti Tun Hussein Onn Malaysia, Parit Raja, 86400 Batu Pahat, Johor, Malaysia.*
[2]*Faculty of Mechanical and Manufacturing Engineeering Technology, Universiti Teknikal Malaysia Melaka, Hang Tuah Jaya, 76100 Durian Tunggal, Melaka, Malaysia.*
[3]*Faculty of Manufacturing Engineeering, Universiti Teknikal Malaysia Melaka, Hang Tuah Jaya, 76100 Durian Tunggal, Melaka, Malaysia.*

[a)] *Corresponding author: izwana@uthm.edu.my*
[b)]*mohamed.saiful@utem.edu.my*
[c)]*hasan@uthm.edu.my*
[d)]*alamin@utem.edu.my*

Abstract. Hydroxyapatite (HAp) from fish by-product exhibits good biocompatibility and bioactivity on implants. The aim of the study is to investigate the elemental composition, crystalline phases, and functional groups of HAp synthesised from *fringescale sardinella* fish bones by heat decomposition method at temperature of 600, 900, and 1200 °C. The synthesised powders were characterized using fourier transform infrared spectroscopy (FTIR), X-ray diffraction (XRD), and energy dispersive spectroscopy (EDS). After calcination of the raw fish bone to 600, 900, and 1200 °C, the FTIR data showed the existence of phosphate and hydroxyl peaks in the calcined fish bones. At 900 and 1200°C, the XRD data observed shows well-defined peaks of HAp pattern. The elemental composition evaluated by EDS provides information on the calcium to phosphate formation into apatite with a Ca/P ratio of 2.80, 0.98, 1.64 and 1.79 atomic % for raw fish bones and calcined samples, respectively. It can be concluded that the *fringescale sardinella* fish bones show promising findings particularly on the synthesisation of HAp for biomedical applications.

INTRODUCTION

Approximately 70% of fish meal and 73.9% of fish oil are made from the the fish catch [1]. The remaining for instance bones, skins, heads and viscera were categorized as by-products. Improper management of the waste can lead to health and environmental problems. Albeit the increasing efforts to convert the by-products into useful commodity, the major amount is still used for animal foods [2,3]. Fish bones contain high amount of valuable mineral phase HAp. Highly biocompatible and bioactive properties with human tissue marked HAp as excellent calcium phosphate-based bioceramic which have been increasingly used and received tremendous attention in the biomedical field in the last decade [4-7]. The presence of important trace element such as zinc, magnesium, natrium, potassium, silicon, and carbonate has made fish waste-derived HAp much more bioactive and biocompatible compared to synthetic apatite [8]. According to the Scopus database, the number of publications that relate to HAp and "biomedical applications" increased more than two-fold between 2012 (99) and 2021 (232) (Fig. 1). In recent technologies, HAp was used as

Advanced Materials Characterization Techniques 2022
AIP Conf. Proc. 2925, 020045-1–020045-6; https://doi.org/10.1063/5.0183935
Published by AIP Publishing. 978-0-7354-4804-9/$30.00

heavy metal remover [9,10], electrodes restoration [11,12], and bone repair [13-15]. In the present study, the extraction of HAp from *fringescale sardinella* fish bones was evaluated by using different calcination temperature. The extracted HAp was characterized using fourier transform infrared (FTIR) spectroscopy, X-ray diffraction (XRD), and energy dispersive spectrometry (EDS) in order to observe the functional groups, crystalline phases, and elemental composition, respectively.

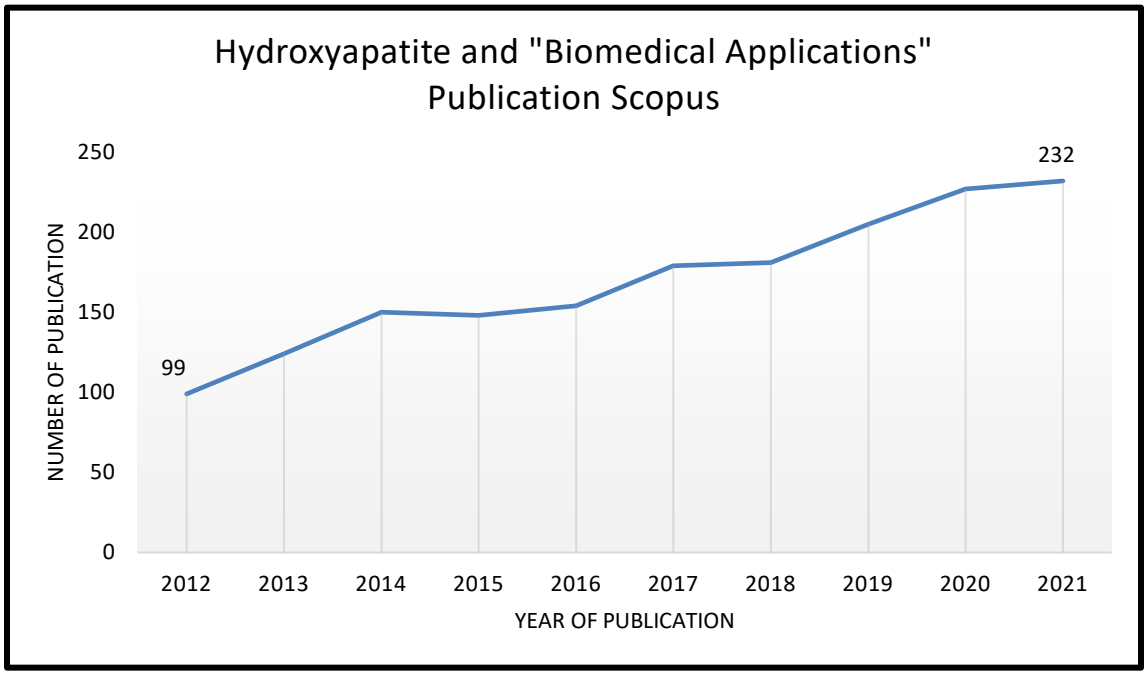

FIGURE 1. Published articles for keyword hydroxyapatite and "biomedical applications" (2012 – 2021)

MATERIALS AND METHODS

Fish wastes were obtained from a fish processing company in Pantai Remis, Perak, Malaysia. The wastes were cleaned thoroughly and then boiled for 1 hour and washed with tap water repeatedly to remove protein and impurities. This was followed by fish bones drying at 100°C in an electric oven for 24 h. The dried fish bones were crushed using a rotor mill at 12,000 rpm to obtain powders prior to calcination. The powders were calcined under atmospheric condition using an electric furnace at 600°C and heating rate of 10°C/min with 3 h of dwelling time. Calcined powders were crushed using ball milling to obtain fine raw powders ready for characterization. Figure 2 shows the experimental procedure for the synthesisation of HAp.

The raw powders were further calcined at 900 and 1200°C to observe the effects of sintering temperature on the crystalline phases, functional groups, and elemental decomposition relating to produced HAp at different calcination temperature. The temperature of 600, 900, and 1200 °C was selected for calcination due to high possibility of obtaining Ca/P stoichiometric molar ratio (1.67) [16-18]. The labelling of synthesised and analysed samples is: RFB (raw fish bone), HA600 (HAp calcined at 600°C), HA900 (HAp calcined at 900°C) and HA1200 (HAp calcined at 1200°C). The elemental composition was observed using energy dispersive spectroscopy (EDS). Phase identification and crystallinity of HAp samples were analyzed using X-ray diffraction (XRD, Bruker D8 Advance, United States). Data was taken from the diffraction angle 2θ between 20° to 80°. The functional groups present in the samples have been identified by fourier transform infrared spectroscopy (FTIR, Perkin Elmer Spectrum 100, United Kingdom) equipped with UATR sampling wavelength in the range of 400-4000 cm^{-1}. Samples were grinded and mixed with dried KBr using ceramic mortar and loaded into a sample holder mounted in the instrument.

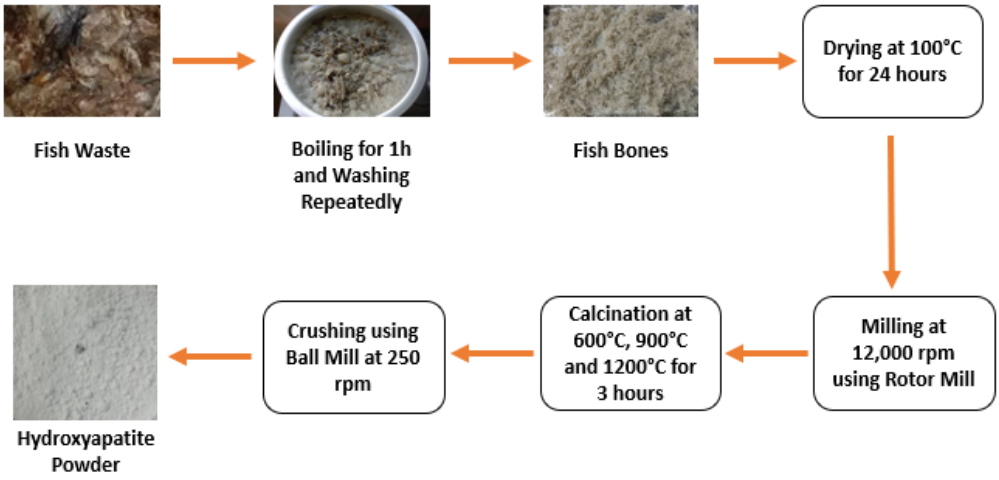

FIGURE 2. Hydroxyapatite preparation

RESULTS AND DISCUSSIONS

The characteristic peaks of calcium and phosphorus are present with the weight and atomic percentages which provides the mean relative calcium to phosphate ratios as shown in Tables 1 and 2. Tables 1 and 2 represent the elemental composition of the raw biowastes and synthesised HAp with their corresponding calcium to phosphate (Ca/P) ratios obtained by energy dispersive spectroscopy (EDS). Weight percentage and atomic percentage were considered to give Ca/P approximations. It was revealed that Ca/P ratios for sample HA900 were 2.12 and 1.64 for weight and atomic percentages respectively. Comparatively, the atomic Ca/P ratio (1.64) of HA900 was the closest to stoichiometric Ca/P ratio (1.67) amongst all the HAp samples investigated in this study. HA600 and HA900 were considered as calcium deficient samples due to the Ca/P ratio of lower than 1.67, while RFB and HA1200 were phosphorus deficient (Ca/P > 1.67). Calcium deficient HAp has Ca/P ratio lower than 1.67 and it has high ability in assisting ion-exchange to various cations [19]. It has been reported that calcium deficient HAp plays essential roles in bone formation and bone remodelling [20]. The Ca/P ratio was higher than 1.67 owing to the exchange of ions such as carbonate in the HAp structure [21]. There was also trace element magnesium detected in HA900 and HA 1200 samples, which is important for bone density and osteoporosis prevention [22,23].

TABLE 1. Calcium/Phosphate Ratio (Weight %)

	Element		
Sample	**Calcium, Ca**	**Phosphorus, P**	**Ca/P**
RFB	12.55	3.46	3.63
HA600	10.10	7.98	1.27
HA900	25.01	11.80	2.12
HA1200	19.11	8.26	2.31

TABLE 2. Calcium/Phosphate Ratio (Atomic %)

	Element		
Sample	**Calcium, Ca**	**Phosphorus, P**	**Ca/P**
RFB	4.62	1.65	2.80
HA600	4.00	4.08	0.98
HA900	11.04	6.74	1.64
HA1200	8.72	4.88	1.79

XRD patterns of HAp powders as shown in Fig. 3 revealed no secondary phases besides HAp. The pattern of the HAp powder obtained at 600 °C is characterized by broad and has poor crystalline structure, that were indexed as diffraction peaks of HAp. Rietveld refinement revealed that the sample of fish bone treated at 600 °C was composed by poorly crystalline HAp. Besides, the samples obtained at 900 and 1200°C are characterized by HAp as the main crystalline phase. The obtained patterns resemble standard HAp powder pattern. A previous study by Rozaini et al. presents almost similar hydroxyapatite pattern at calcination temperature of 900°C [24].

Parallel to the increase of calcination temperature, the HAp contained in the samples derived from *fringescale sardinella* fish bones displays more intense and sharper peaks. This reveals an increase of structural order and crystal growth upon increase of calcination temperature. In terms of crystallinity, *fringescale sardinella* fish bones samples treated at 900°C and 1200ºC are very similar to a commercial HAp material, presenting narrow and well-defined peaks.

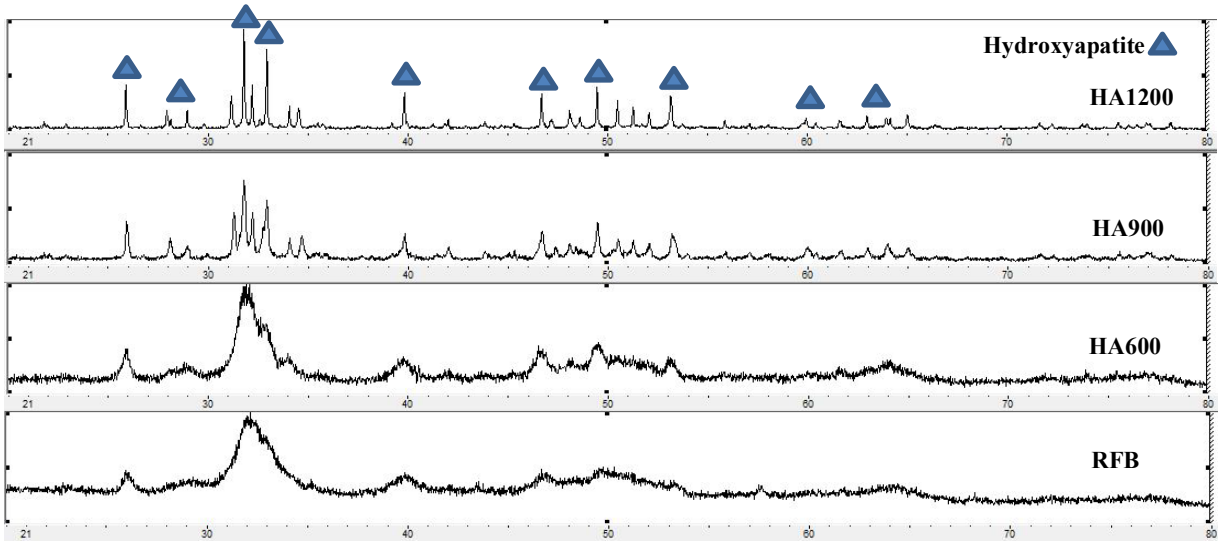

FIGURE 3. XRD Patterns of Hydroxyapatite Powder – RFB, HA600, HA900, HA1200

Figure 4 shows the fourier transform infrared (FTIR) spectrogram of synthesised HAp of RFB and calcined fish bone powders. Typical characteristic bands corresponding to the carbonate groups of the $CaCO_3$ component of HAp are located around 1465 cm^{-1} and 1535 cm^{-1}. The bands at 568.9 and 601.7 cm^{-1} corresponds to bending mode of PO_4 group [25]. The prominent band for all samples at 3450 cm^{-1} is due to the vibratory stretching of OH group of HAp while the bands at 1631 cm^{-1} was attributed to adsorbed water molecules. The bands at 1631 cm-1 and 3450 cm-1 for all samples with broader band for RFB and HA600 samples correspond to the disappearance of absorbed water after sintering [26,27].

The wavenumber with an explicit peak at 3575 cm^{-1}, and a weaker peak at 630 cm^{-1} corresponded to the stretching and bending vibrations of the hydroxyl in the molecular structure of HAp. The sintered sample showed frequency bands around 2326 and 2360 cm^{-1} ascribed to the release of CO_2 during heat treatment [28]. The formative indicator of HAp at all point of calcination (600, 900, 1200°C) was in the form of pronounced broad bands around 1000-1100 cm^{-1} can be ascribed to asymmetric stretching mode of vibration of PO4 group. Nevertheless, a small band noticed at 945 cm^{-1} for RFB indicates a deficient asymmetric stretching mode of vibration of phosphate group that was made pronounced by heat treatment.

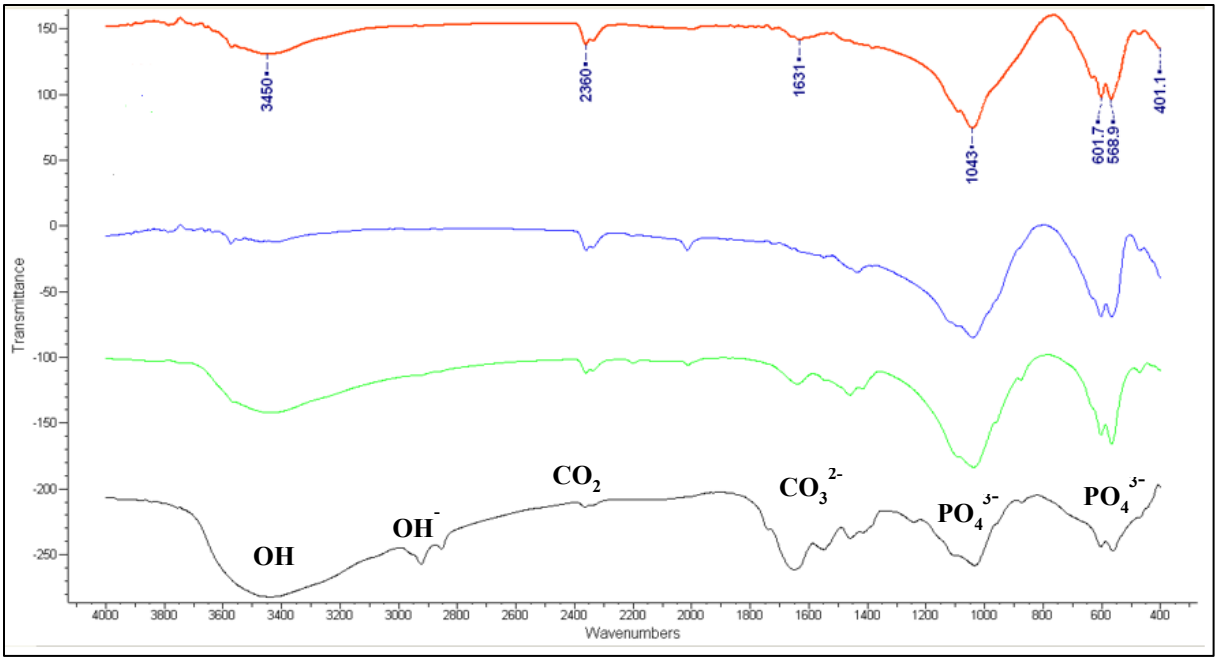

FIGURE 4. FTIR spectra for RFB, HA600, HA900, and HA1200 powder

CONCLUSIONS

Natural HAp from *fringescale sardinella* fish bones was synthesised using the calcination method. This is a low-cost method for the formation of HAp. According to EDS analysis, composition of powder from HA900 (1.64) is closer to the ideal stoichiometric Ca/P ratio (1.67) for HAp. XRD pattern of HA900 and HA1200 fit very well with the typical XRD pattern for HAp with narrow and well-defined peaks. FTIR results confirmed the presence of a carbonated group (preferable for biomedical applications). The successful characterization of this important nanomaterial will be useful in biomedical applications, especially in bone tissue engineering through its development. This material may reduce the environmental effect of by-products from the fish processing industry while efficiently safeguarding industrial pollution and waste management. This research suggests that *fringescale sardinella* fish bones is an alternative biomaterial with promising potential for biomedical applications in the field of bone tissue engineering.

ACKNOWLEDGMENTS

This research was supported by the Ministry of Higher Education (MOHE) via Fundamental Research Grant Scheme (FRGS/1/2018/STG07/UTHM/02/6). The authors would also like to thank the Faculty of Mechanical and Manufacturing Engineering, Universiti Tun Hussein Onn Malaysia for its support.

REFERENCES

1. E.B. Claude, A.M. Aaron and P.D. Robert, Food Security **14**, 805-827 (2022).
2. M. Afreen and I. Ucak, Journal of Survey in Fisheries Sciences **6(2)**, 55-64 (2020).
3. Tugiyono, G.F. Indra, P. Yuwana and Suharso, Pakistan Journal of Biological Sciences **23(5)**, 701-707 (2020).
4. M.S.F. Hussin, A.M. Serah, K.A. Azlan, H.Z. Abdullah, M.I. Idris, I. Ghazali, A.H.M. Shariff, N. Huda and A.A. Zakaria, Polymers **13**, 647 (2021).
5. N.A.S.M. Pu'ad, P. Koshy, H.Z. Abdullah, M.I. Idris and T.C. Lee, Heliyon **5**, e01588 (2019).

6. S.L. Bee and Z.A.A. Hamid, Ceramics International **46**, 17149-17175 (2020).
7. M.S.F. Hussin, H.Z. Abdullah, M.I. Idris and M.A.A. Wahap, Heliyon **8(8)**, e10356 (2022).
8. A.F.S. Paola, S.G. Belarmino, C.G.G. Beatriz, R.P. Elisabeth and J.A.A. Pedro, Revista Materia **23(4)**, e-12217 (2018).
9. D. Nunez, J.A. Serrrano, A. Mancisidor, E. Elgueta, K. Varaprasad, P. Oyarzun, R. Caceres, W. Ide and B.L. Rivas, RSC Advances **9**, 22883-22890 (2019).
10. A. Nayak and B. Bhushan, Materials Today: Proceedings **46(20)**, 11029-11034 (2021).
11. M. Zhang, S. Cai, S. Shen, G. Xu, Y. Li, R. Ling and X. Wu, Journal of Alloys and Compounds **658**, 649-656 (2016).
12. W.C. Lin, C.C. Chuang and P.T. Wang, Materials **12(1)**, 116 (2019).
13. D. Mingzu, C. Jingdi, L. Kaihua, X. Huaran and S. Cui, Composites Part B: Engineering **215**, 108790 (2021).
14. F. Zeyu, C. Jinjie, Z. Bin, G.F.S. Steve, and L. Kaili, Journal of Orthopaedic Translation **28**, 118–130 (2021).
15. V.S. Kattimani, S. Kondaka and K.P. Lingamaneni, Bone and Tissue Regeneration Insights **7**, 9-19 (2016).
16. A.R.S. Nurhidatyat, A.P. Bayuseno, R. Ismail and R.B. Taqriban, Journal of Biomedical Science and Bioengineering **1(1)**, 27-31 (2021).
17. M. Boutiguiza, J. Pou, R. Comesana, F. Lusquino, A.D. Carlos, and B. Leon, Material Science and Engineering C **32**, 478-486 (2012).
18. J. Ventakesan and S.K. Kim, Materials **3(10)**, 4761-4772 (2010).
19. N. Atsushi, N. Kentaro, N. Chiya, M. Hidenobu and M. Katsuyuki, Materials Sciences and Applications **2**, 1194-1198 (2011).
20. G. Maria-Pau, E. Montserrat, M. Yassine, B. Victor and P. David, EFORT Open Reviews **3(5)**, 173-183 (2018).
21. S. Rui-Xue, L. Yao, N. Yu-Rong, Z. Xiao-Hui, C. Dong-Shan, T. Jian, S. Xian-Chang and C. Ke-Zheng, Ceramics International **43**, 16792-16798 (2017).
22. S. Castiglioni, A. Cazzaniga, W. Albisetti and J.A.M. Maier, Nutrients **5(8)**, 3022-3033 (2013).
23. M. Rondanelli, M.A. Faliva, A. Tartara, C. Gasparri, S. Perna, V. Infantino, A. Riva, G. Petrangolini and G. Peroni, Biometals **34**, 715-736 (2021).
24. M.Z.H. Rozaini, H. Hamzah, M.H. Razali, U.M. Osman, C.P. Wai, S.K.C. Soh, S.R. Ghazali, N.H. Ibrahim and L.C. Fei, Asian J Agric & Biol **7**, 33-47 (2019).
25. P. Szterner and M. Biernat, Bioinorganic Chemistry and Applications 3481677 (2022).
26. R. Nawang, M.Z. Hussein, K.A. Matori, C.A.C. Abdullah and M. Hashim, Results in Physics **15**, 102540 (2019).
27. E.A. Ofudje, A.I. Adeogun, M.A. Idowu and S.O. Kareem, Heliyon **5(5)**, e01716 (2019).
28. S. Ummartyotin and B. Tangnorawich, Colloid Polym. Sci. **293(9)**, 2477-2483 (2015).